Electrocatalytic Activity of Ti/Al/Ti/PbO$_2$-WC Rod Composite Electrodes During Zinc Electrowinning

Huixi Li, Zhen Chen[*]*, Qiang Yu, Wei Zhu, and Wenrong Cui*

Faculty of science, Kunming University of Science and Technology, Kunming 650093,
People's Republic of China
[*]E-mail: chenzhen69@qq.com

Ti/Al/Ti/PbO$_2$-WC rod composite electrodes and Ti/PbO$_2$-WC composite electrodes were prepared by pulse current electrodeposition in a lead nitrate solution that contains WC microparticles, and the electrocatalytic activity of Ti/Al/Ti/PbO$_2$-WC rod composite electrodes was emphasized. The surface microstructure was characterized by scanning electron microscopy (SEM), and the electrocatalysis of the oxygen evolution behavior was investigated using anodic polarization curves and cyclic voltammetry curves in a synthetic zinc electrowinning electrolyte of 50 g·L^{-1} Zn^{2+} and 150 g·L^{-1} of H$_2$SO$_4$ at 40°C. The results show that applying the Ti/Al/Ti rod substrate can clearly decrease the grain size of the PbO$_2$ electrodes, and the surface of electrodes become more compact. Compared with the titanium substrate electrode, applying the Ti/Al/Ti rod substrate can obviously increase the exchange current density j^0 of the PbO$_2$-WC composite electrode during the process of oxygen evolution, reduce the apparent activation energy E_a of the oxygen evolution reaction, increase the values of electric double layer capacitance C$_{dl}$ during the charging process, and improve the electrocatalytic stability. Employing the Ti/Al/Ti rod as the substrate of a composite electrode can effectively improve the electrode coating microstructure, increase the electrocatalytic activity of the oxygen evolution reaction in the electrolytic zinc liquid and exert positive effects on the application of the new substrate composite electrode.

1. INTRODUCTION

Lead dioxide electrodes have been widely used as anode materials and play an important role in wastewater treatment, metallurgy and other fields on account of their high electric catalytic activity, good electrical conductivity, higher electrochemical stability, corrosion resistance in different solution, etc.[1-5]. Titanium is widely used as the substrate for lead dioxide electrodes due to its good corrosion

resistance and because its thermal expansion coefficient is similar to that of lead dioxide[6]. The traditional lead-silver alloy anode used for zinc metallurgy will be superseded by the Ti/PbO_2 anode due to its longer lifetime, lower energy consumption, higher current efficiency and better product quality[7]. To further improve the catalytic performance of PbO_2 electrodes, various functional particles (such as RuO_2, TiO_2, CeO_2, ZrO_2 and WC) were applied[8-15], and interlayers were added (such as SnO_2-Sb_2O_3, α-PbO_2, SnO_2-Sb)[16-18]. However, there are few reports on the improvement of the electrode performance from changing the substrate state.

Titanium reserves are rich, cheap, and also have good processing properties[19] and good corrosion resistance, and the thermal expansion coefficient is similar to PbO_2, so it is widely applied as the PbO_2 electrode substrate[6]. However, the biggest drawback of titanium is its high resistivity as a base metal, as its resistivity of 0.42 μΩ · m is 17 times that of aluminum. Some researchers have prepared Ti/Al/Ti substrate composite electrode, the inner layer of which is made of aluminum, and the outer layers of which are covered by titanium[20]. Their studies show that the Ti/Al/Ti plate has a lower resistivity and better conductivity than a Ti plate and, as the substrate of the composite electrode, can effectively reduce the evolution overpotential[21]. Nevertheless, in the field of metallurgy, using a Ti/Al/Ti rod as the substrate of PbO_2 composite electrode is rarely reported.

In this paper, based on the abovementioned information, Ti/Al/Ti/PbO_2-WC rod composite anodes were prepared via pule current electrodeposition of a mixed $Pb(NO_3)_2$ and $Cu(NO_3)_2$ hydrosolvent. Ti/PbO_2-WC composite anodes were also prepared under the same conditions to compare with it. The effects of the substrate on the composite electrode coating microstructure were investigated using SEM. Anodic polarization curves and cyclic voltammetry were applied to investigate the electrocatalytic properties of composite electrodes in electrolytic zinc liquid. Lastly, the electrocatalytic stability of the composite electrodes was evaluated by chronoamperometry (CA).

2. EXPERIMENTAL METHODS

2.1 Electrode preparation

2.1.1 Ti plates and Ti/Al/Ti rods pretreatment

The Ti plates (10 mm × 50 mm × 1 mm) and Ti/Al/Ti rods (10 mm × 50 mm × 10 mm) were polished by 320-grit paper strips and then cleaned using ultrasound for 20 minutes to remove sand particles lodged in the metal. Then, the Ti plates and Ti/Al/Ti rods were treated by etching in boiling aqueous 15% oxalic acid for nearly 2 hours until the TiO_2 was thoroughly dissolved, followed by thorough washing with doubly distilled, de-ionized water. At this point, Ti plates and Ti/Al/Ti rods were gray and had lost their metallic sheen.

2.1.2 Ni interlayer preparation

The Ni interlayer deposited onto the pretreated Ti plates and Ti/Al/Ti rods was prepared by DC deposition in which 40.0 g of $NiSO_4$, 2.5 g of NaCl, 10.0 g of H_3BO_3 and 20.0 g of Na_2SO_4 were

dissolved in 300 mL of distilled water as the electrolyte, the Ti plates and Ti/Al/Ti rods served as the cathode, and the stainless steel was used as the anode. Then, the samples were electroplated at 40°C for 10 min at a current density of 75 mA·cm^{-2}.

2.1.3 Composite electrodes preparation

The Ti/PbO$_2$-WC and Ti/Al/Ti/PbO$_2$-WC composite electrode materials were prepared via pulse electrodeposition; the Ti plates and Ti/Al/Ti rods served as the anodes, and the stainless steel was used as a cathode. The composition of the plating bath was 210 g·L^{-1} of Pb(NO$_3$)$_2$; 0.5 g·L^{-1} of NaF; 25 g·L^{-1} of Cu(NO$_3$)$_2$; 0.5 g·L^{-1} of AEO (fatty alcohol polyoxyethylene); and 40 g·L^{-1} of WC (average size: 1-3 μm). The operating conditions were as follows: the pulse average current density was 30 mA·cm^{-2}, the duty cycles were set to 30%, the pulse frequency was 20 Hz, the bath temperature was 50°C, the magnetic stirring rate was 600 rpm, and the electrodeposition time was 60 minutes.

2.2 Electrode performance testing

An electrochemical workstation (CHI660D, China) with three electrode systems was used during measurements of the anodic polarization curves, cyclic voltammetry curves and chronoamperometry in a synthetic zinc electrowinning electrolyte of 50 g·L^{-1} Zn^{2+} and 150 g·L^{-1} of H$_2$SO$_4$ at 40°C. The working electrodes were the Ti/PbO$_2$-WC composite electrodes and Ti/Ai/Ti/PbO$_2$-WC composite electrodes with working areas of 1.0 cm^2. A saturated calomel electrode (SCE) was used as the reference electrode, and the counter electrode was platinum, with an area of 1.0 cm^2. Anodic polarization curves were measured at a sweep rate of 10 mV·s^{-1} between 0.8 V and 2.1 V, and the anodic polarization curves at different temperatures (30-50°C) were also measured to obtain the apparent activation energy (E_a). The cyclic voltammetry (CV) curves were recorded between 1.55 V and 1.65 V (in a purely capacitive potential region) with scan rates of 20-100 mV·s^{-1}. Chronoamperometry (CA) measurements were carried out at a potential of 1.8 V (in the oxygen evolution reaction potential region) for 3 h.

Moreover, a Phenom ProX Scanning Electron Microscope (SEM) was applied to observe the microscopic surface morphology of the as-prepared Ti/PbO$_2$-WC composite electrode and Ti/Ai/Ti/PbO$_2$-WC composite electrode, and the phase structure of the two composite electrodes was analyzed using X'pert Powder X-ray diffraction (XRD).

3. RESULTS AND DISCUSSION

3.1 Physical characterization

3.1.1 Surface morphology using SEM

Fig. 1 shows the microscopic morphology of the two different composite electrode surfaces magnified 5000 times. The results show that after using the Ti/Al/Ti rod substrate, the electrode

surface morphology significantly changes when compared with that of the Ti/PbO$_2$-WC electrode (Fig. 1a). The electrode surface microstructure is compact, interface bonding is tight, the grain size of PbO$_2$ is clearly smaller, and intergranular arrangement is compact, which can increase the specific surface area of the electrode. The presented structure is attributed to the better conductivity of the Ti/Al/Ti rod substrate; when the conductivity of the substrate is increased, the electron transfer rate inside the electrode is accelerated and the exchange rate of the electrode surface charge is also increased, which results in the an increased deposition rate of lead dioxide and refined PbO$_2$ grain sizes[20].
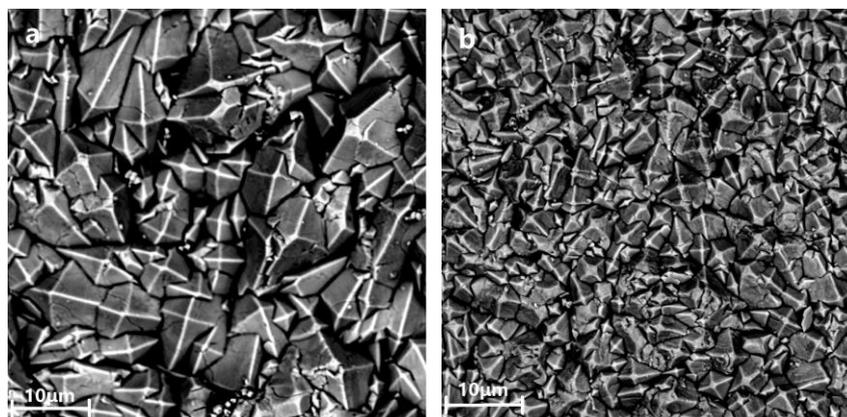

Figure 1. Surface morphology of (a)Ti/PbO$_2$-WC composite electrode and (b)Ti/Al/Ti/PbO$_2$-WC composite electrode.
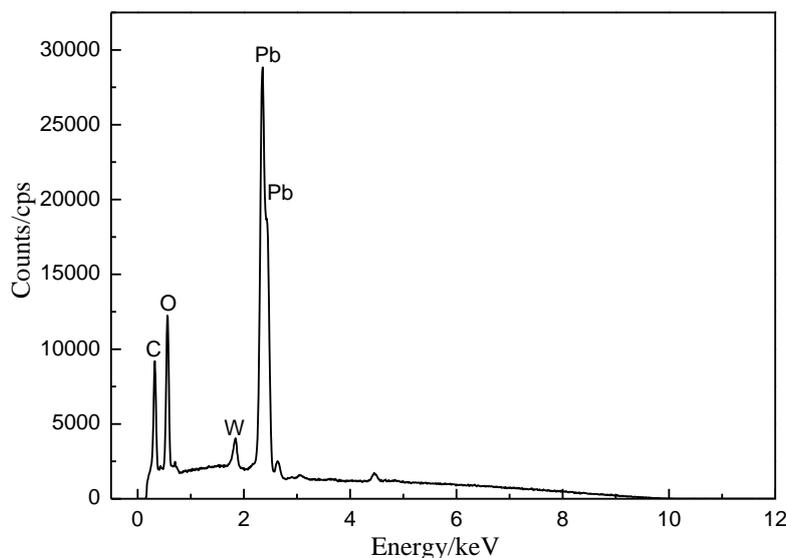
3.1.2 Elemental analysis using EDS

Figure 2. Energy spectrogram analysis results using mapping scanning for the Ti/Al/Ti/PbO$_2$-WC composite electrode

As we can see, Fig. 2 shows the EDS analysis result via mapping scanning of the Ti/Al/Ti/PbO$_2$-WC electrode. Four elements (oxygen, lead, tungsten, and carbon) are shown in the EDS spectrogram, indicating that the composite coating consists mainly of lead dioxide and tungsten carbide.

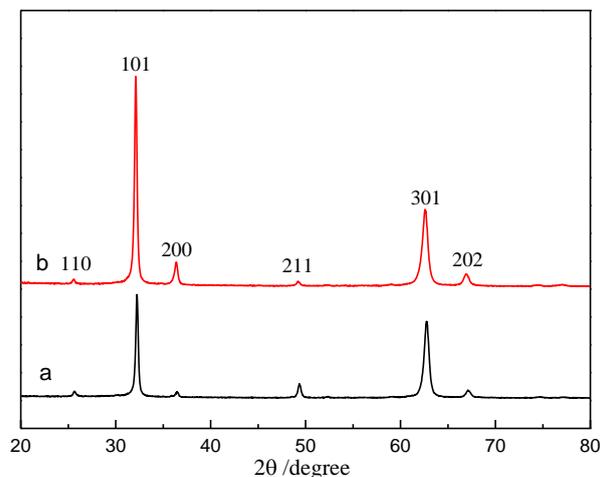### 3.1.3 Composition analysis using XRD

Figure 3. XRD patterns of (a)Ti/PbO$_2$-WC composite electrodes and (b)Ti/Al/Ti/PbO$_2$-WC composite electrodes.

X-ray diffraction (XRD) was applied to study the phase composition of PbO$_2$-WC anodes obtained with different substrates, and the results are shown in Fig. 3. It is important to note that the peaks are intense at 25.4°, 31.9°, 36.3°, 49.1°, 62.5°, and 66.7° in both samples, and all of them are indexed to the tetragonal-shaped β-PbO$_2$ (PDF 41-1492). Obvious differences can be found by comparing the two curves. The peaks belonging to electrode b at 31.9°, 36.3° and 66.7° are stronger than those of electrode a, but the peak at 49.1° is weaker. It can be seen that the changing of the substrate can influence the growth orientation of the crystal face. As we can see from Fig. 3, the peak width of the Ti/Al/Ti/PbO$_2$-WC electrode increases compared with that of the Ti/PbO$_2$-WC electrode. In addition, we can conclude that the grain size of the PbO$_2$ coating decreases after using the Ti/Al/Ti rod substrate because the width of the diffraction peak is inversely proportional to the grain size[22]. That is, the adoption of the Ti/Al/Ti rod substrate can refine the grains, which results in a denser PbO$_2$ coating.

3.2 Anodic polarization curves

3.2.1 Tafel characterization

In this paper, the corrected potential (E_c) was used to present the real potential value of OER. The anodic polarization curve for the Tafel analysis was corrected using formula (1)[23]:

$$E_c = E_{appl} - iR_s \qquad (1)$$

where E_{appl} is the applied potential, i is the faradaic current and R_s is the uncompensated electrolyte resistance. Fig. 4 shows the iR_s corrected anode polarization curves of the PbO$_2$-WC composite anodes with different substrates. The overpotential value (η) used for the fitted Tafel lines of oxygen evolution was obtained from part of the anodic polarization curves based on the following formula (2)[1,24]:
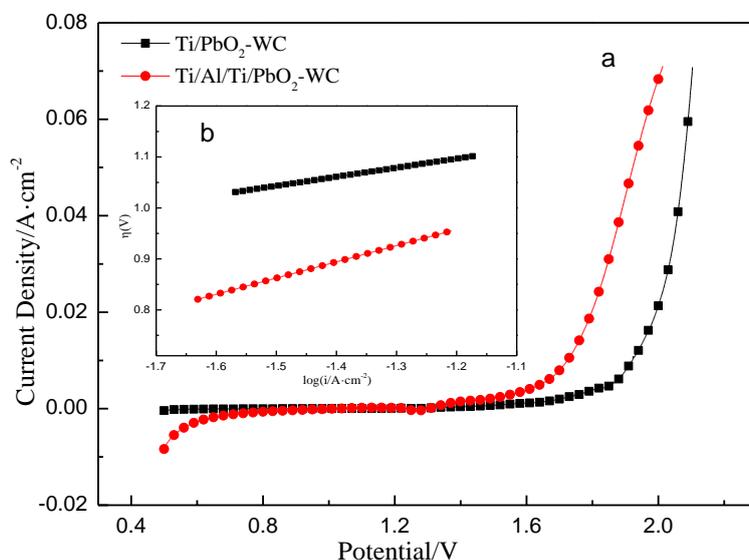
$$\eta=E_c+0.231V-1.240V \qquad (2)$$

Figure 4. Anode polarization curves and Tafel linear fitting curves of Ti/PbO$_2$-WC composite electrode and Ti/Al/Ti/PbO$_2$-WC composite electrode.

where E_c(SCE) is the corrected potential, 0.231 V (NHE) is the potential of the SCE, and 1.240 V (NHE) is the reversible potential of oxygen evolution, calculated from the Nernst equation using a synthetic zinc electrowinning electrolyte of 50 g·L^{-1} of Zn^{2+} and 150 g·L^{-1} of H$_2$SO$_4$ at 40°C.

The iR_s-corrected Tafel lines (η-log i) of the anode samples obtained with different substrates in the plating bath are shown in Fig. 4b. The potential intercepts and slope values of the two lines were analyzed by Origin 8.5 software, and the results are shown in Table 1. The η listed in Table 1 was calculated using the Tafel formula (3)[25] as follows:

$$\eta=a+b\log i \qquad (3)$$

where η and i respectively represent the overpotential of oxygen evolution and the Faradaic current, while a and b are the constants obtained through linear fitting of the relationship curve of η and log i in the Origin 8.5 software.

The electrode surface (exchange) current density j^0 can be calculated using the Tafel equation (3) when the overpotential of oxygen evolution $\eta=0$.

According to electrochemical theory, electrode polarization and the reversibility of electrode reactions can be evaluated using j^0. In general, a higher j^0 implies that the electrode is not easily polarized, the electrode has better reversibility, and the electrode reaction occurs more easily. As

shown in Table 1, after applying the Ti/Al/Ti substrate, the exchange current density j^0 increases a lot, indicating that the electrode with Ti/Al/Ti substrate has better electrocatalytic activity.

The overpotentials η were identified as one of the most important criteria for OER, as shown in Table 1, and η obviously reduced after applying the Ti/Al/Ti substrate, which shows that the coating was more conducive to the OER. In short, after using the Ti/Al/Ti substrate, the oxygen evolution potential (SCE) and η obviously decrease, whereas j^0 increases. This depolarization can be attributed to the better conductivity of the Ti/Al/Ti substrate.

Table 1. Oxygen evolution kinetics parameters of composite electrodes

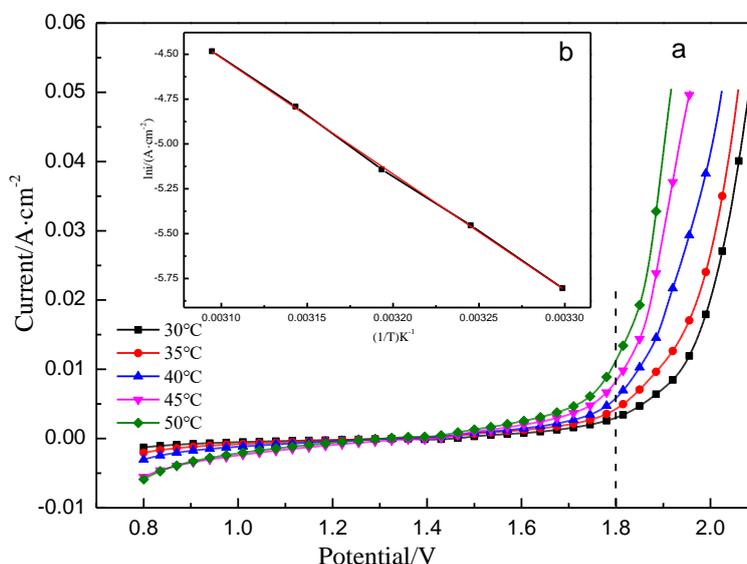|	a(V)	b(V·dec^{-1})	j^0(A·cm^{-2})	η(V)
Ti/PbO$_2$-WC	1.311	0.178	4.446×10^{-8}	0.990
Ti/Al/Ti/PbO$_2$-WC	1.340	0.318	6.171×10^{-5}	0.722

3.2.2 Activation energy E_a

Figure 5. a. Ti/PbO$_2$-WC composite electrode polarization curves at different electrolyte temperatures; b. lni-T^{-1} linear fitting curve

It is known that whether the reaction occurs easily or not can be characterized by activation energy. Lowering the activation energy is a common feature of a catalytic reaction. Generally, lower activation energy suggested better catalytic performance of the composite electrode. The activation energy (E_a) can be determined using the Arrhenius equation[26-28] by plotting the working electrode anodic polarization curve at different temperatures (T),

$$\ln i = \ln A - \frac{E_a}{RT} \qquad (4)$$

where A is the pre-exponential factor, R is the gas constant (8.314 mol^{-1}K^{-1}), T is the absolute temperature, and E_a is the molar activation energy.
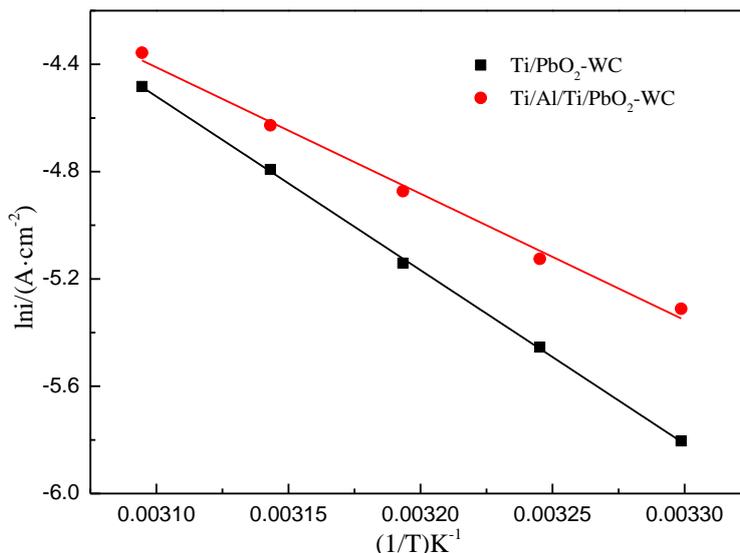

Figure 6. Arrhenius plots of the two composite electrodes

As we can see, Fig. 5a shows the anodic polarization curves at different temperatures (30-50°C) of the Ti/PbO$_2$-WC composite electrode, the chart of ln$i$-T^{-1} has been plotted (as shown in Fig. 5b), and the activation energy can be calculated by the slope of the straight line.

There is an obvious relationship between the activation energy and the oxygen evolution reaction. The smaller the activation energy is, the easier it is for the anode oxygen evolution reaction to occur. The Arrhenius plots of the composite electrodes prepared with different substrates are shown in Fig. 6. The different values of the slope (ln$i$-T^{-1}) infer the different activities of the composite electrodes in the process of OER, and the corresponding activation energy values are listed in Table 2. As shown in Table 2, the activation energy of the electrode with a Ti substrate is 53.83 kJ/mol. However, it obviously decreases and has a lower value of 39.16 kJ/mol after employing the Ti/Al/Ti rod substrate, indicating that the composite electrode has better catalytic activity. This corroborates the conclusion of the anodic polarization curve analysis. Using the Ti/Al/Ti rod substrate can effectively reduce the oxygen evolution reaction activation energy, owing to the good electrical conductivity of the new substrate.

Table 2. Activation energy E_a of the two composite electrodes

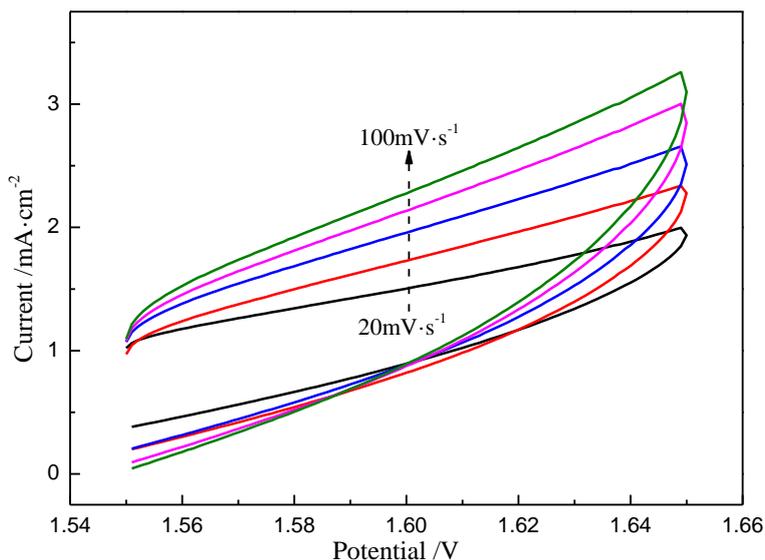|	**Ti/PbO$_2$-WC**	**Ti/Al/Ti/PbO$_2$-WC**
E_a**(kJ/mol)**	53.83	39.16

3.3 Electric double layer capacitance

Figure 7. Voltammetric curves of the Ti/PbO$_2$-WC composite electrode at different scan rates in the capacitive potential region (1.55-1.65 V)
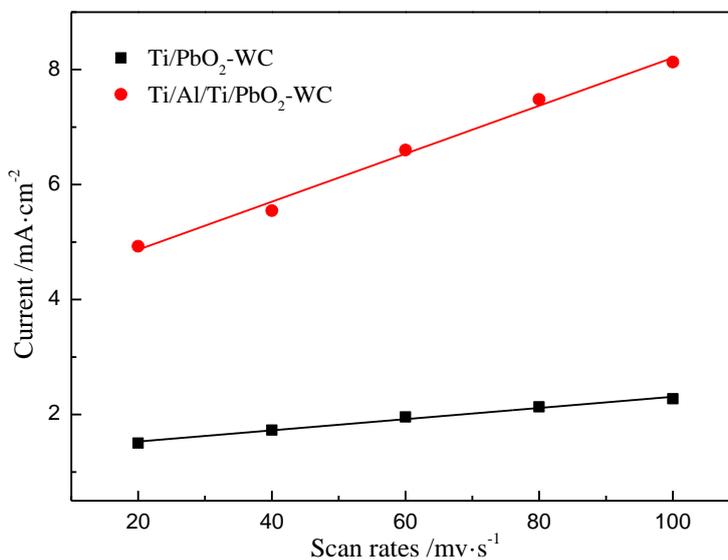

Figure 8. Plots of the current density at 1.60 V vs. the scan rate.

Previous studies have proven that the electrochemically active surface area is directly proportional to the number of active sites of the catalyst for the OER, and the active surface area can be evaluated using the electrochemical double-layer capacitance (C$_{dl}$)[15,29-31]. To further study the effects of different substrates on the amount of coating surface active sites of the catalyst for the OER, the narrow potential of the double layer capacitive potential area was selected, and cyclic voltammograms were tested at different scan rates. As shown in Fig. 7, a purely capacitive potential region has been selected from 1.55 V to 1.65 V, in which only the non-Faraday charging process

occurs. For all composite electrodes, voltammetric curves were recorded between 1.55 V and 1.65 V as a function of scan rate, v ($5 \leq v \leq 100$ mV·s^{-1}), and the current, i_E, was measured at constant potential (E=1.60 V). The double-layer capacitance was obtained from the slope of i_E vs. v graphics[31,32]. Fig. 7 shows the voltammetric curve of the Ti/PbO$_2$-WC composite electrode obtained in the plating solution, recorded in the capacitive potential region (between 1.55 V and 1.65 V) at different scan rates, and the i_E vs. v graphic of the two composite electrodes is shown in Fig. 8.

The double-layer capacitance (C_{dl}) values of the two composite electrodes are shown in Table 3. It can be seen from Table 3 that the C_{dl} of Ti/Al/Ti/PbO$_2$-WC (41.73 mF cm^{-2}) is almost 4-fold higher than that of the Ti/PbO$_2$-WC (9.74 mF cm^{-2}). The results confirm that the surface of the Ti/Al/Ti/PbO$_2$-WC electrode has a much larger number of active sites, which significantly contribute to its excellent OER activity. This is attributed to the better electrical conductivity of the Ti/Al/Ti rod substrate, which makes the electron transfer rate inside the electrode accelerated and increases the exchange rate of the electrode surface charge, which increases the deposition rate of lead dioxide and ensures that the nucleation rate of PbO$_2$ is greater than the growth rate. Thus, the coating is able to have smaller grain size and larger actual surface area, which has a positive impact on the electric double-layer capacitance value.

Table 3. Double-layer capacitance values of different composite electrodes

	Ti/PbO$_2$-WC	Ti/Al/Ti/PbO$_2$-WC
C_{dl}(mF·cm^{-2})	9.74	41.73

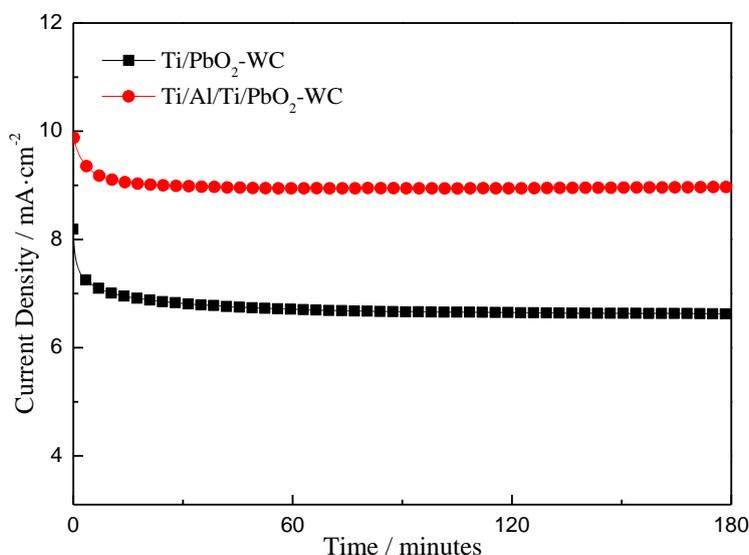*3.4 Electrocatalytic stability tested using chronoamperometry*

Figure 9. Chronoamperometric curves obtained on the two composite electrodes in the synthetic zinc electrowinning electrolyte

To evaluate the electrocatalytic stability of the composite electrodes for the oxygen evolution reaction under long-term operation, chronoamperometric (CA) measurements were carried out at 1.8 V (vs. SCE) inside the oxygen evolution reaction potential region for 3 h. The CA curves for composite electrodes with different substrates in the synthetic zinc electrowinning electrolyte at 1.8 V are shown in Fig. 9. As seen, the shape of the CA curves obtained with different substrates is similar. The currents dropped rapidly at first and then became relatively stable in the two CA curves. The initial high current corresponds mainly to double layer charging[33]. As shown in Fig. 9, the transient current density becomes higher after employing the Ti/Al/Ti substrate; that is to say, the OER rate of the composite electrode is becoming faster, indicating that the catalytic performance of the composite electrodes is improved after the adoption of the new substrate. A stable current plateau indicates a stable trace of OER activity[34]. The more stable the current plateau of the CA curves is, the better is the catalytic stability of the electrode. The current plateau of the Ti/Al/Ti/PbO_2-WC electrode is more stable, and the CA curve has higher transient current density, suggesting that the electrode has good catalytic stability and better catalytic performance. The similar results are also shown in our former study[15].

4. CONCLUSION

1. PbO_2-WC composite electrodes were prepared via pule current electrodeposition with different substrates. SEM and XRD analyses show that applying the Ti/Al/Ti rod substrate obviously reduces the grain size of the PbO_2-WC composite electrode, and the electrode surface becomes more compact. Compared with the Ti/PbO_2-WC composite electrode, the Ti/Al/Ti/PbO_2-WC rod composite electrode has a uniform and close microstructure, a smaller grain size and fewer surface microstructure defects.

2. Compared with the Ti/PbO_2-WC composite electrode, the Ti/Al/Ti/PbO_2-WC rod composite electrodes demonstrate lower oxygen evolution overpotential η, higher exchange current density j^0 and lower activation energy E_a. Meanwhile, the value of the electric double-layer capacitance C_{dl} in the charging process is greater by four times that of the titanium substrate electrode. Moreover, its electrocatalytic stability improves.

References

1. H. Yang, B. Chen, H. Liu, Z. Guo, Y. Zhang, X. Li, and R. Xu, *International Journal of Hydrogen Energy*, 39 (2014) 3087.
2. Y. Yao, H. Dong, L. Jiao, N. Yu, and L. He, *Journal of the Electrochemical Society*, 163 (2016) D179.
3. Y. Yao, M. Zhao, C. Zhao, andW. Xiao, *Journal of the Electrochemical Society*, 160 (2013) D553.
4. M. Xu, Z. Wang, F. Wang, P. Hong, C. Wang, X. Ouyang, C. Zhu, Y. Wei, Y. Hun, and W. Fang, *Electrochimica Acta*, 201 (2016) 240.
5. Q. Li, Q. Zhang, H. Cui, L. Ding, Z. Wei, and J. Zhai, *Chemical Engineering Journal*, 228 (2013) 806.

6. X. Xie and Z. Guo, The research progress of Ti—based PbO$_2$, electrode, *in The National Academic Communication of Electronic Electroplating and Surface Treatment*, Shanghai, China, (2009).
7. W. Yan, Z. Chen, Q. Yu, W. Zhu, H. Wang, and B. Du, *Journal of the Electrochemical Society*, 163 (2016) D414.
8. R. Amadelli, L. Samiolo, A. B. Velichenko, V. A. Knysh, T. V. Luk'Yanenko, and F. I. Danilov, *Electrochimica Acta*, 54 (2009) 5239.
9. G. Li, J. Qu, X. Zhang, and J. Ge, *Water Research*, 40 (2006) 213.
10. M. Musiani, F. Furlanetto, and R. Bertoncello, *Journal of Electroanalytical Chemistry*, 465 (1999) 160.
11. Y. Song, G. Wei, and R. Xiong, *Electrochimica Acta*, 52 (2007) 7022.
12. A. B. Velichenko, V. A. Knysh, T. V. Luk'yanenko, Y. A. Velichenko, and D. Devilliers, *Materials Chemistry and Physics*, 686 (2012) 131.
13. G. M. Pajonk and T. Manzalji, *Catalysis Letters*, 21 (1993) 361.
14. Y. Yao, C. Zhao, and J. Zhu, *Electrochimica Acta*, 69 (2012) 146.
15. H. Li, Z. Chen, Q. Yu, W. Zhu, and W. Cui, *Journal of the Electrochemical Society*, 164 (2017) H1064.
16. Y. Yao, M. Zhao, C. Zhao, H. Zhang, *Electrochim Acta* 117 (2014) 453.
17. Q. Qiao, Q. Li, D. Yu, H. Liang, *Chinese Journal of Applied Chemistry*, 17(2000).
18. H. Bi, C. Yu, W. Gao, P. Cao, *Electrochimica Acta,* 113 (2013) 446.
19. Y. Hu, L.Chen, *Electropiating & Finishing*, 22 (2003) 58
20. X. Yang, P. Zhu, W. Huang, S. Zhou, J. Xu, J. Xu, H. Ma, *Transactions Of Materials And Heat Treatment*, 31 (2010) 15.
21. J. Zhang, P. Zhu, J. Dai, S. Zhou, Y. Cao, *Rare Metal Materials And Engineering*, 44 (2015) 1459.
22. K. T. Kawagoe and D. C. Johnson, *Journal of the Electrochemical Society*, 141 (1994) 3404.
23. Y. Lai, Y. Li, L. Jiang, W. Xu, X. Lv, J. Li, and Y. Liu, *Journal of Electroanalytical Chemistry*, 671 (2012) 16.
24. R. D. Xu, L. P. Huang, J. F. Zhou, P. Zhan, Y. Y. Guan, and Y. Kong, *Hydrometallurgy*, 22 (2012) 1693
25. Phd M. Schlesinger, *Modern Electroplating [M]*. 4thed. The Electro-chemical Society Inc, (2014)) New York, America.
26. D. Wilmer, *Berichte Der Bunsengesellschaft/physical Chemistry Chemical Physics*, 100 (1996) 180.
27. M. Zhou, Q. Dai, L. Lei, C. A. Ma, and D.Wang, *Environmental Science & Technology*, 39 (2005) 363.
28. S. Tong, T. Zhang, and M. A. Chun'An, *Chinese Journal of Chemical Engineering*, 16 (2008) 885.
29. C. Z. Yuan, Y. F. Jiang, Z. Wang, X. Xie, Z. K. Yang, A. B. Yousaf, and A. W. Xu, *Journal of Materials Chemistry A*, 4 (2016) 8155.
30. M. A. Lukowski, A. S. Daniel, F. Meng, A. Forticaux, L. Li, and S. Jin, *Journal of the American Chemical Society*, 135 (2013) 10274.
31. M. H. P. Santana, L. M. D. Silva, and L. A. D. Faria, *Electrochimica Acta*, 48 (2003) 1885.
32. C. L. P. S. Zanta, A. R. D. Andrade, and J. F. C. Boodts, *Electrochimica Acta*, 44 (1999) 3333.
33. H. Razmi, E. Habibi and H. Heidari, *Electrochimica Acta*, 53 (2008) 8178.
34. H. Jin, S. Mao, G. Zhan, F. Xu, X. Bao, and Y. Wang, *Journal of Materials Chemistry A, 3* (2017) 1078.